

Superhalogen properties of $CumCln$ clusters: Theory and experiment

Y. J. Ko, H. Wang, K. Pradhan, P. Koirala, A. K. Kandalam et al.

Citation: *J. Chem. Phys.* **135**, 244312 (2011); doi: 10.1063/1.3671457

View online: <http://dx.doi.org/10.1063/1.3671457>

View Table of Contents: <http://jcp.aip.org/resource/1/JCPSA6/v135/i24>

Published by the [American Institute of Physics](#).

Related Articles

Rigorous formulation of two-parameter double-hybrid density-functionals

J. Chem. Phys. **135**, 244106 (2011)

Diferrocenyl oligothiophene wires: Raman and quantum chemical study of valence-trapped cations

J. Chem. Phys. **135**, 234705 (2011)

Inhomogeneous fluids of colloidal hard dumbbells: Fundamental measure theory and Monte Carlo simulations

J. Chem. Phys. **135**, 234510 (2011)

Studies on the structure, stability, and spectral signatures of hydride ion-water clusters

J. Chem. Phys. **135**, 214308 (2011)

The excitation function for $Li+HFLiF+H$ at collision energies below 80 meV

J. Chem. Phys. **135**, 204306 (2011)

Additional information on *J. Chem. Phys.*

Journal Homepage: <http://jcp.aip.org/>

Journal Information: http://jcp.aip.org/about/about_the_journal

Top downloads: http://jcp.aip.org/features/most_downloaded

Information for Authors: <http://jcp.aip.org/authors>

ADVERTISEMENT

AIPAdvances

Submit Now

Explore AIP's new
open-access journal

- Article-level metrics now available
- Join the conversation! Rate & comment on articles

Superhalogen properties of Cu_mCl_n clusters: Theory and experiment

Y. J. Ko,¹ H. Wang,¹ K. Pradhan,² P. Koirala,³ A. K. Kandalam,^{3,a)} K. H. Bowen,^{1,a)} and P. Jena^{2,a)}

¹Department of Chemistry and Material Sciences, Johns Hopkins University, Baltimore, Maryland 21218, USA

²Department of Physics, Virginia Commonwealth University, Richmond, Virginia 23284, USA

³Department of Physics, McNeese State University, Lake Charles, Louisiana 70609, USA

(Received 18 August 2011; accepted 30 November 2011; published online 30 December 2011)

Using a combination of density functional theory and anion photoelectron spectroscopy experiment, we have studied the structure and electronic properties of CuCl_n^- ($n = 1-5$) and Cu_2Cl_n^- ($n = 2-5$) clusters. Prominent peaks in the mass spectrum of these clusters occurring at $n = 2, 3$, and 4 in CuCl_n^- and at $n = 3, 4$, and 5 in Cu_2Cl_n^- are shown to be associated with the large electron affinities of their neutral clusters that far exceed the value of Cl. While CuCl_n ($n \geq 2$) clusters are conventional superhalogens with a metal atom at the core surrounded by halogen atoms, Cu_2Cl_n ($n \geq 3$) clusters are also superhalogens but with $(\text{CuCl})_2$ forming the core. The good agreement between our calculated and measured electron affinities and vertical detachment energies confirm not only the calculated geometries of these superhalogens but also our interpretation of their electronic structure and relative stability. © 2011 American Institute of Physics. [doi:10.1063/1.3671457]

I. INTRODUCTION

Superhalogens are clusters or molecules, which are composed of a central metal atom surrounded by halogen atoms. They form when the number of halogen atoms exceeds the normal valence of the metal atom. Their electron affinities (EAs), which measure the energy gained when an electron is attached to a neutral species, are much larger than that of a halogen atom. Vertical detachment energy (VDE) which measures the energy difference between an anion and its neutral, both at the ground state geometries of the anion, have been found to reach values as high as 14 eV.¹ Bartlett and co-workers showed that PtF_6 molecules can ionize an O_2 molecule or Xe atom^{2,3} and estimated the EA of PtF_6 to be 6.8 eV. Boldyrev and Gutsev later coined the word superhalogen⁴⁻⁶ and outlined conditions a system should satisfy to in order for its EA to be large. Because of the importance of negative ions in chemistry as oxidizing agents,⁷ there is growing interest in the design and synthesis of new superhalogen molecules. Recently, research has also focused on the use of superhalogens as building blocks of energetic materials capable of destroying biologically active materials.⁸ About a decade ago, the smallest superhalogens, MX_2 ($M = \text{Li, Na, and Cu; X = Cl, Br, and I}$) were studied by photoelectron spectroscopy (PES) and analyzed by *ab initio* calculations.^{9,10} Later, larger superhalogens MX_3 ($M = \text{Be, Mg, and Ca; X = Cl, Br, and F}$) (Refs. 11–13) and MX_4 ($M = \text{B and Al; X = F, Cl, and Br}$) (Refs. 14 and 15) have been studied. Note that the metal atoms are monovalent in MX_2 , divalent in MX_3 , and trivalent in MX_4 . Clusters with more than one metal atom such as $\text{Na}_x\text{Cl}_{x+1}$ ($x = 1-4$) (Ref. 16) and Mg_2F_5 (Ref. 17) have also been found to be superhalogens.

While most of the prior work on superhalogens has concentrated on *sp* metal atoms, recent studies have focused on transition and coinage metal atoms as the central core. Examples of the latter class of superhalogens include MnO_4 (Ref. 18), CrO_4 (Ref. 19), and ScCl_4 (Refs. 20 and 21) whose EAs are 5.0 eV, 4.96 eV, and 6.84 eV, respectively, while the metal hexafluorides include AuF_6 , PtF_6 , (Refs. 22 and 23) second- and third-row transition metal fluorides,^{24,25} and coinage metal fluorides²⁶ have been reported recently. In a recent study,²⁶ superhalogens consisting of coinage metal atoms surrounded by F atoms, MF_n ($M = \text{Cu, Ag, Au, } n = 1-7$) was studied systematically. For $n \geq 2$, these clusters possess superhalogen properties and as many as six F atoms can be bound to a single Au atom. However, in the case of Cu, the maximum numbers of F atoms that bind atomically to the Cu is four. For example in CuF_5 cluster, two of the F atoms dimerize and then weakly bind to the CuF_3 portion of the cluster. In the case of anions, the fragmentation energy of CuF_5^- was found to be four times smaller than that of CuF_4^- cluster. Unfortunately, there are no experimental data to compare with theory since F is difficult to handle in experiments. Consequently, we carried out a combined theoretical and experimental study of the Cu_mCl_n clusters ($m = 1, 2; n = 1-5$).

Cu usually exists in monovalent (I) and divalent (II) states and hence can easily bind up to two halogen atoms. Since it was shown earlier²⁶ that up to four F atoms can be bound chemically to a neutral Cu atom and CuF_n clusters ($n \geq 2$) are superhalogens, a natural question arises: can a single Cu atom also bind up to four Cl atoms and have large EA? Using hybrid density functional theory (DFT) based calculations we studied CuCl_n clusters up to $n = 5$. The calculated fragmentation energies of neutral and anionic CuCl_5 clusters are very small indeed and suggest that larger CuCl_n clusters ($n \geq 6$) will not be energetically very stable. We will show later that this is consistent with the mass spectra of CuCl_n clusters. All CuCl_n clusters are stable and those with $n \geq 2$ are

^{a)}Authors to whom correspondence should be addressed. Electronic addresses: kbrown@jhu.edu; akandalam@mcneese.edu; and pjena@vcu.edu.

superhalogens. Using our pulsed arc cluster ion source (PACIS) we produced Cu clusters, which were then allowed to react with Cl. We not only observed CuCl_n^- species up to $n = 6$ but also clusters composed of Cu_2 at the core. We have confined our anion PES studies to CuCl_n clusters with $n = 1-4$. The calculated EAs and VDEs are compared with the corresponding measured values using anion PES, to verify the ground state geometries of anion and establish the superhalogen properties of these clusters. In Sec. II we provide a brief description of our theoretical and experimental procedure. The results are discussed in Sec. III and summarized in Sec. IV.

II. THEORETICAL AND EXPERIMENTAL METHODS

The ground state geometries of neutral and anionic Cu_mCl_n clusters were obtained by hybrid DFT based electronic structure calculations using GAUSSIAN 03 program.²⁷ The hybrid density functional²⁸ B3LYP along with 6-311++G (3d) basis set was used for all the calculations. Different initial geometries with halogen atoms bound to the Cu atom(s) both molecularly and chemically were considered for geometry optimization to identify the ground state structures of these clusters. Different possible spin multiplicities were considered for each of the isomers to determine the preferred spin state of these clusters. The convergence for total energy and gradient were set to 10^{-9} Hartree and 10^{-4} Hartree/Å, respectively. The vibrational frequencies of all the clusters studied are positive and thus the structures are confirmed to belong to minima on the potential energy surface. The zero-point vibrational energy (ZPVE) is not included in the calculations of EAs or fragmentation energies.

Our experimental anion PES study is conducted by crossing a beam of mass-selected negative ions with a fixed frequency photon beam and energy analyzing the resultant photodetached electrons. The photo-detachment process is governed by the energy-conserving relationship, $h\nu = \text{EBE} + \text{EKE}$, where $h\nu$ is the photon energy, EBE is the electron binding energy, and EKE is the electron kinetic energy. The main information obtained is the electronic energy spectrum of the anion's corresponding neutral at the structure of the anion. Thus, even though these experiments are performed on negative ions, their results pertain to their neutral counterparts as well.

Our apparatus has been described previously.²⁹ In brief, the apparatus consists of an ion source, a linear time-of-flight mass selector, a photo-detachment laser, and a magnetic bottle photoelectron spectrometer (MB-PES). The instrumental resolution of the MB-PES is 35 meV at 1 eV EKE. An ArF excimer laser (193 nm, 6.424 eV) was used to photodetach the cluster anions of interest. Photoelectron spectra were calibrated against the known atomic lines of Cu^- . In this study, Cu_mCl_n anions were generated with a PACIS that has been described in detail elsewhere.³⁰ In brief, a discharge is triggered between two copper rods serving as anode and cathode, vaporizing sample from the cathode. About 2 bar of ultrahigh purity chlorine gas is back-filled into the discharging region. Then, a 30–40 μs long 150 V pulse is applied to the anode causing a discharge between the electrodes in which

chlorine gas partially dissociates (generating a momentarily high concentration of Cl atoms) and copper atoms are vaporized. About 10 bar of helium gas flushes the chlorine-copper plasma mix down a 20 cm flow tube, where it reacts, cools, and forms clusters. The source was operated at 10 Hz repetition rate.

III. RESULTS AND DISCUSSIONS

A. CuCl_n ($n = 1-5$) clusters: Theory

We first discuss our results of a single Cu atom interacting with Cl atoms to see how the geometries and electronic structures evolve with the addition of each Cl atom. The ground state geometries of neutral and anionic CuCl_n ($n = 1-5$) clusters are shown in Figure 1. The geometries of neutral clusters are similar to their corresponding anions for $n = 1$ and 2. While the geometries of neutral and anion cluster for $n = 3$ are slightly different, they differ considerably for $n = 4$. In neutral CuCl_3 cluster, we found three iso-energetic, nearly identical isomers that differ in the Cl–Cl bond distances (Fig. 1, 3a–3c). The lowest energy structure has C_{2v} symmetry, with a weak interaction between two chlorine atoms (Fig. 1, 3a). The bond length between the two chlorine atoms is 2.69 Å, which is 32.5% larger than the Cl–Cl bond length (2.03 Å) in a Cl_2 dimer. A highly symmetric D_{3h} structure (Fig. 1, 3b) in which there is no Cl–Cl interaction is found to be only 0.05 eV higher in energy. The quasi-molecular bonding between two Cl atoms in Fig. 1(3a) suggests that Cu is in +II oxidation state while atomic bonding of all Cl atoms in Fig. 1(3b) suggests that Cu is in +III oxidation state. A third isomer (C_{2v} symmetry) without any interaction

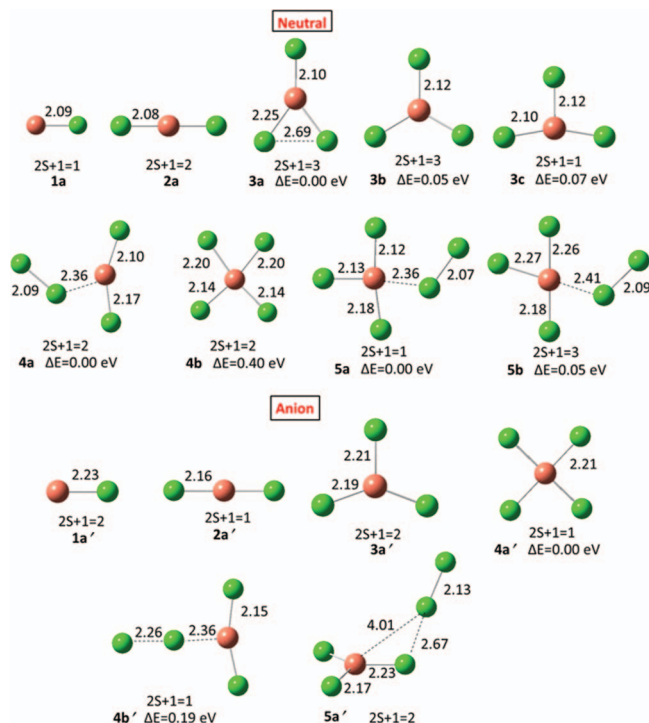


FIG. 1. The lowest energy and few higher energy isomers of neutral and anionic CuCl_n clusters. The green spheres represent chlorine atoms, while the red spheres are copper atoms. All the bond lengths are given in Angstroms.

between the halogen atoms as in Fig. 1 (3b) but with singlet spin multiplicity is 0.07 eV higher in energy (Fig. 1, 3c). The first two isomers prefer a triplet spin state ($2S+1 = 3$). The above small energy differences are within the computational uncertainty (~ 0.20 eV) of the current level of theory and neutral CuCl_3 can exist in either of these spin states. The ground state geometry of CuCl_3^- cluster has C_{2v} symmetry with two distinct Cu–Cl bond lengths of 2.21 and 2.19 Å (Fig. 1, 3a') and prefers a doublet spin state.

In neutral CuCl_n clusters with $n \geq 4$, two of the halogen atoms form molecule-like structure while the remaining bind atomically to Cu. For example, in the neutral CuCl_4 cluster (Fig. 1, 4a) two of the chlorine atoms form a Cl_2 dimer, which in turn binds to the Cu atom. Thus, one can consider neutral CuCl_4 as $(\text{CuCl}_2)\text{Cl}_2$ cluster. The fragmentation analysis of the CuCl_n clusters, discussed later, shows Cl_2 and CuCl_2 as the most preferred fragmentation products of CuCl_4 cluster indicating that CuCl_4 is indeed a $(\text{CuCl}_2)\text{Cl}_2$ complex. In the case of anionic CuCl_4 cluster, however, a planar structure (Fig. 1, 4a') with all the four halogen atoms binding atomically to the central Cu atom (D_{4h} symmetry) is found to be lowest in energy. Another planar isomer, in which a weakly bonded Cl_2 interacting with CuCl_2 moiety is found to be 0.19 eV higher in energy (Fig. 1, 4b'). Since the energy difference between these two isomers is less than the accuracy of our computational method (~ 0.2 eV), both these structures are possible for CuCl_4^- cluster. Interestingly, in the case of neutral CuCl_4 cluster, the D_{4h} symmetric structure is found to be 0.40 eV higher in energy than the ground state structure containing Cl_2 molecule (Fig. 1, 4b). The ground state geometries of CuCl_5 and CuCl_5^- clusters can be viewed as $(\text{CuCl}_3)\text{Cl}_2$ and $(\text{CuCl}_3^-)\text{Cl}_2$ complexes (Fig. 1, 5a and 5a'), respectively. The anionic CuCl_5 cluster prefers a doublet ($2S+1 = 2$) spin state, while in the case of neutral CuCl_5 cluster, both singlet and triplet spin multiplicities are found to be energetically very close, with the singlet lower in energy by 0.05 eV. Since CuCl_5 exists as $(\text{CuCl}_3)\text{Cl}_2$ complex, the spin multiplicity scenario discussed in CuCl_3 , i.e., singlet and triplet spin states being close in energy, is also reflected in CuCl_5 cluster. The average bond lengths of the anionic clusters are larger than the neutral clusters for $n = 1$ and 2 while both species have the same average bond length for $n = 3, 4$, and 5.

Based on the ground state geometries of neutral and anionic CuCl_n clusters, one can conclude that the maximum oxidation state of Cu is +3 in these clusters. Interestingly, in our earlier theoretical work on coinage-metal fluoride clusters, it has been shown that Cu can have a maximum oxidation state of +4. This difference in the oxidation states of Cu atom in these two systems (chloride vs. fluorides) can be understood from the fact that fluorine is more electronegative than chlorine and the metal atoms can reach a higher oxidation state when interacting with fluorine. The thermodynamic stability of the neutral and anionic CuCl_n clusters against fragmentation into $\text{CuCl}_{n-1} + \text{Cl}$ and $\text{CuCl}_{n-2} + \text{Cl}_2$ units are calculated by the following equations:

$$\Delta E_{\text{neutral}} = -[E(\text{CuCl}_n) - E(\text{CuCl}_{n-m}) - E(\text{Cl}_m)],$$

$$m = 1, 2, \quad (1)$$

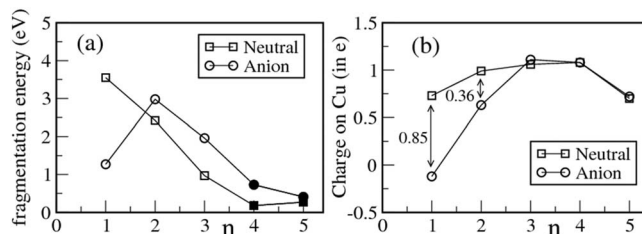


FIG. 2. Calculated (a) fragmentation energies (in eV): filled symbols show that the preferable channel consist of a Cl_2 molecule rather than atomic Cl (see the text for the preferred channels for each cluster) and (b) charge on Cu atom in CuCl_n clusters.

$$\Delta E_{\text{anion}}^1 = -[E(\text{CuCl}_n^-) - E(\text{CuCl}_{n-m}^-) - E(\text{Cl}_m)],$$

$$m = 1, 2, \quad (2a)$$

$$\Delta E_{\text{anion}}^2 = -[E(\text{CuCl}_n^-) - E(\text{CuCl}_{n-m}^-) - E(\text{Cl}_m^-)],$$

$$m = 1, 2. \quad (2b)$$

For computation of the fragmentation energies of the anionic clusters, one has to further take into account the possibility that the extra charge can be carried either by Cl or by the Cu–Cl complex. In principle, the preferred fragmentation channel should have the lowest reaction barrier. However, in the absence of such studies, we consider the channel for which ΔE is minimum as the preferred channel. The fragmentation energies associated with the minimum energy channel for each cluster are plotted in Figure 2(a). Neutral clusters prefer to dissociate into a CuCl_{n-1} and Cl for $n = 1-3$. The most preferable fragmentation channel for CuCl_n ($n = 4$ and 5) clusters is $\text{CuCl}_{n-2} + \text{Cl}_2$. The corresponding fragmentation energies are calculated to be 0.18 eV and 0.27 eV for CuCl_4 and CuCl_5 , respectively. These small fragmentation energies further reinforces the fact that CuCl_n ($n = 4$ and 5) clusters exist as $(\text{CuCl}_{n-2})\text{Cl}_2$ complexes. In the case of anionic CuCl_n clusters, the negative charge resides on the Cl atom for $n = 1$, while in the cases of CuCl_n^- ($n \geq 2$) clusters the extra charge resides on the CuCl_{n-1} fragment. For $n = 2-3$, the most preferred fragmentation channel is found to be $\text{CuCl}_{n-1}^- + \text{Cl}$; on the other hand, for $n = 4$ and 5, fragmentation leading to Cl_2 and CuCl_{n-2}^- is the most preferred channel. This transformation of the preferred fragmentation product from Cl to Cl_2 at $n = 4$ can be understood from the fact that CuCl_2^- is the most stable cluster in the anionic series (see Fig. 2(a)) and thus, the CuCl_4^- prefers to dissociate into CuCl_2^- cluster and Cl_2 but not to $\text{CuCl}_3^- + \text{Cl}$. The preferred fragmentation path for CuCl_5^- is consistent with the fact that this cluster forms a $(\text{CuCl}_3^-)\text{Cl}_2$ complex and thus will fragment into Cl_2 and CuCl_3^- . The fragmentation energy for this channel is calculated to be 0.40 eV. Note that a similar transition in the preferred fragmentation channel was observed in CuF_n clusters,³¹ where beyond $n = 3$, fragmentation into CuF_{n-2} and F_2 was preferred over other channels.

The calculated VDE values of CuCl_n^- clusters and EA values of CuCl_n clusters are given in Table I. The EA of Cl

TABLE I. Theoretical and experimental EAs of Cu_mCl_n ($m = 1, 2; n = 1-5$) clusters and VDEs of Cu_mCl_n^- ($m = 1$ and $2; n = 1-5$) clusters. All values are given in eV.

Cluster (m_B)	Calculated		Experimental	
	EA (eV)	VDE (eV)	EA (eV)	VDE (eV)
CuCl	1.44	1.54		
CuCl ₂	4.27	4.35	4.3 ± 0.1	4.6 ± 0.1
CuCl ₃	5.27	5.65	5.5 ± 0.1	5.8 ± 0.05
CuCl ₄	4.82	5.28	4.6 ± 0.1	5.0 ± 0.05
CuCl ₅	5.64	5.94		
Cu ₂ Cl ₂	1.87	2.67		
Cu ₂ Cl ₃	4.79	4.99	5.0 ± 0.2	5.2 ± 0.05
Cu ₂ Cl ₄	4.58	4.72	4.6 ± 0.1	4.8 ± 0.1
Cu ₂ Cl ₅	5.15	5.99		

is 3.6 eV and is the highest among all the elements in the periodic table. Apart from CuCl, EA for all other clusters are larger than that of the Cl atom and hence are classified as superhalogens. To understand the superhalogen properties we have analyzed the total charge on the Cu and Cl atoms as a function of n for both neutral and anionic CuCl_n clusters using natural bond orbital (NBO) analysis.³¹ The results are plotted in Fig. 2(b). In all neutral CuCl_n clusters, the total charge on Cu atoms is positive indicating that charge is transferred from Cu to the Cl atoms. In anionic clusters, the extra electron either goes to compensate the positive charge on the Cu atom or is distributed over the Cl atoms. In the case of CuCl^- , majority of the electron's charge goes to positively charged Cu and thus results in a low EA. On the other hand, in the case of the CuCl_2^- a large part (74%) of the extra electron's charge is distributed over two Cl atoms. This results in a large EA for CuCl_2 and makes it a superhalogen. In larger CuCl_n clusters, addition of an extra electron does not change the charge on the Cu, implying that the electron's charge is again distributed among all the halogen atoms, rather than the positively charged metal center. The delocalization of the electron's charge over the halogen atoms results in the superhalogen behavior of CuCl_n ($n \geq 2$) clusters. The calculated VDE and EA values (see Table I) are close to each other for $n = 1$ and 2 due to the similarity in their ground state geometries while the difference is significant for $n = 3, 4$, and 5.

Since the lowest energy structures of neutral and negatively charged CuCl_4 cluster are different and there exist two isomers in anion that are close in energy ($\Delta E = 0.19$ eV), in addition to the EA, we have calculated the adiabatic detachment energy (ADE) and VDE for both the anionic isomers. The ADE value was obtained by calculating the energy difference between the ground state geometry of the anionic cluster and the structurally similar isomer of its neutral counterpart. In cases where the ground state geometries of neutral and anionic clusters are similar, the ADE of the anionic cluster is equal to the EA of the corresponding neutral cluster. In the case of CuCl_4^- , the calculated ADE for the lowest energy isomer (Fig. 1, 4a') corresponds to 5.22 eV, while the ADE for the higher energy isomer (Fig. 1, 4b') is calculated to be 4.64 eV. The corresponding VDEs of these two isomers are 5.29 and 5.36 eV, respectively. The EA, the energy differ-

ence between the lowest energy anion and neutral isomers, of CuCl_4 cluster is 4.82 eV. On comparing our calculated values with that of the measured values (see Table I), we conclude that both the isomers (Fig. 1, 4a' and 4b') are contributing towards the PES spectrum.

The superhalogen property of CuCl_2 and CuCl_3 is consistent with the oxidation state of +1 and +2 of the Cu atom. Cu also has been known³² to have an oxidation state of +3 and hence CuCl_4 is also a superhalogen. But large EA of CuCl_5 cannot be directly connected to the oxidation state of Cu. Since CuCl_5 cluster exists as $(\text{CuCl}_3)\text{Cl}_2$ complex, the large EA (5.64 eV) of this cluster is actually a reflection of the EA of CuCl_3 (5.27 eV) moiety. In CuCl_5 , the oxidation state of Cu is +3 but not +5. Note that a similar scenario was observed in our previously reported work²⁶ on CuF_n clusters. Thus, studying the reaction of a metal atom with halogen atoms and measuring their EAs allow a unique way to characterize the oxidation state of metals.

1. CuCl_n ($n = 2-4$) clusters: Experiment

To verify our theoretical prediction, we have carried out experimental studies of Cu clusters interacting with chlorine. In Fig. 3 we show the mass spectrum of Cu_mCl_n^- clusters. In the CuCl_n^- series ($n = 2-6$), we see that the peaks of CuCl_2^- and CuCl_3^- are more intense than any other peaks. While both kinetic and thermodynamic effects play important roles in the intensity distribution in the mass spectrum, conspicuous peaks in mass spectra of Na and other clusters have been successively interpreted³³ on the basis of their relative stability. For example, clusters with even number of electrons tend to be more stable than those with odd number of electrons due to shell closing. In a PACIS source, clusters are usually produced as charged species. In this sense, CuCl_n^- clusters with even number of Cl atoms should be more stable than those with clusters containing odd number of Cl atoms, if the clusters

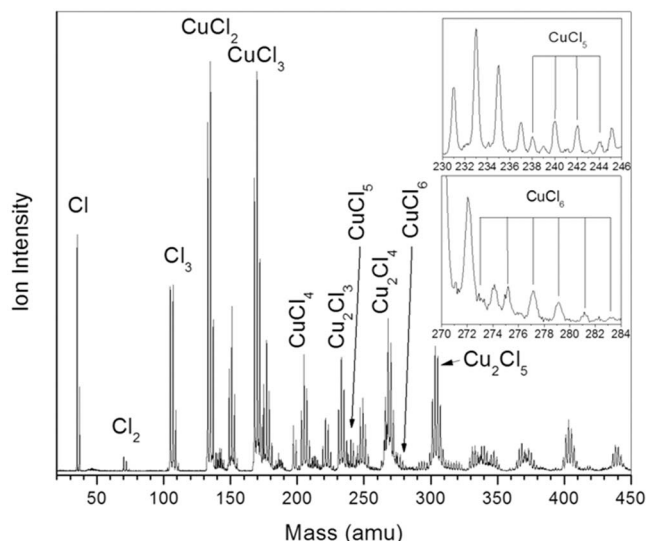


FIG. 3. Typical mass spectrum of Cu_mCl_n^- clusters generated in PACIS. The insets show selected magnified portions of the mass spectrum, revealing the expected isotope patterns.

are born as anions. Reverse is the case if they are born neutral. However, the peak intensities of both CuCl_2^- and CuCl_3^- are about the same. We will show in the following that the enhanced stabilities of these anion clusters are due to the superhalogen properties of their neutral counterparts, which allow them to bind an electron with energies much larger than that of the EA of the Cl atom. The small intensity of the CuCl_5^- peak is consistent with our calculated ground state geometry of this cluster and its small fragmentation energy.

To demonstrate the role of superhalogen character of neutral clusters in the stability of their anionic counterparts, we have measured the EA of CuCl_n clusters and VDE of their corresponding anionic clusters by anion PES. The former is the energy difference between the ground state of the anion and corresponding neutral while the VDE is the energy difference between the ground state of the anion and its neutral at the anion ground state energy. When these geometries remain fairly unchanged after the removal of the extra electron, the photoelectron spectrum remains sharp and EA and VDE are very close to each other.

In Figure 4, we show the photoelectron spectra of CuCl_n^- ($n = 2-4$) clusters. The measured EA and VDE are compared with our calculated results in Table I. Note that the agreement is very good and validates not only the theoretical procedure but also the structure of the clusters. Most interesting in these data is of course the large EAs of CuCl_n ($n = 2-4$) clusters.

The prominent peaks in the mass spectrum in Fig. 3 of these clusters can be partly attributed to their thermodynamic stability. Note that the peak intensity of CuCl_2^- is larger than that of CuCl_4^- . This is consistent with the result that the energy gain in adding a Cl to CuCl^- cluster is 2.98 eV while that in going from CuCl_3^- to CuCl_4^- is only 1.06 eV. In addition, the near identical EA values of CuCl_2 and CuCl_4 clusters can be due to the fact that the neutral CuCl_2 cluster is in fact a

$(\text{CuCl}_2)\text{Cl}_2$ complex and the CuCl_2 unit of this complex is contributing towards the PES spectrum of the CuCl_4 .

2. Comparison of CuCl_n with CuF_n

Recently, a systematic theoretical study²⁶ of the EAs of CuF_n clusters was reported. Although no experimental studies on this system have been carried out, it is interesting to compare the structure and EAs of the two systems as both F and Cl are halogen atoms. We note that in CuF_n^- or CuCl_n^- clusters up to four F or Cl atoms can be bound directly to the Cu atom. In CuF_5^- cluster, four of the F atoms can be bound to Cu atom directly while only three of Cl atoms are bound to Cu atom in CuCl_5^- cluster. The main reason for this differing behavior is that the binding energy of Cl_2 molecule, namely 2.28 eV, is larger than the binding energy of F_2 , namely, 1.52 eV. The equilibrium geometries of CuF_n and CuCl_n clusters are also different. In neutral CuF_n clusters, F atoms are atomically bound to Cu for $n \leq 4$ while two of the F atoms are bound molecularly in CuF_5 . In contrast, in CuCl_n clusters up to only three Cl atoms are bound atomically to the Cu. The fourth Cl atom in neutral CuCl_4 is interacting with one of the Cl atoms rather than the Cu atom. Geometry of CuCl_5 is similar to the CuF_5 cluster. We also note that the EAs of CuF_n are 1.59, 3.79, 5.86, 6.91, and 6.87 for $n = 1, 2, 3, 4,$ and 5 , respectively. These are larger than those shown in Table I for the corresponding CuCl_n system.

B. Cu_2Cl_n ($n = 2-5$) clusters

In addition to the CuCl_n peaks in the mass spectrum in Fig. 3, we also see peaks for Cu_2Cl_3^- and Cu_2Cl_4^- clusters. To understand the stability of these clusters we have measured the photoelectron spectra which are shown in Figure 5. We note that the ADE and VDE of these clusters are also large and they too belong to the superhalogen series. However, unlike the conventional superhalogens discussed above that have only one metal atom at the core, the above superhalogens have two Cu atoms. It is relevant to mention that similar superhalogens consisting of multiple metal atoms have been

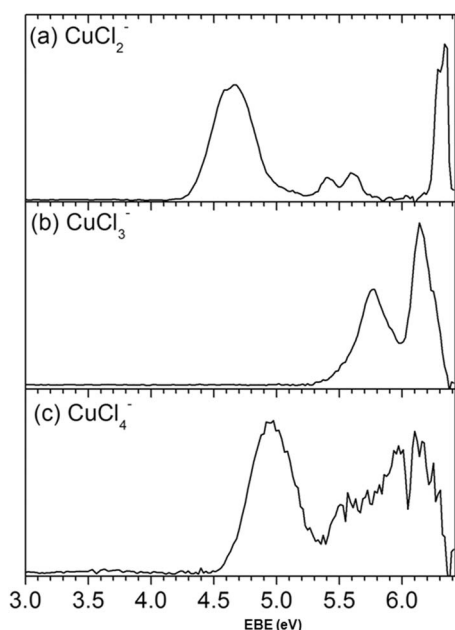


FIG. 4. Photoelectron spectra of CuCl_n^- ($n = 2-4$) cluster anions recorded with 193 nm photons.

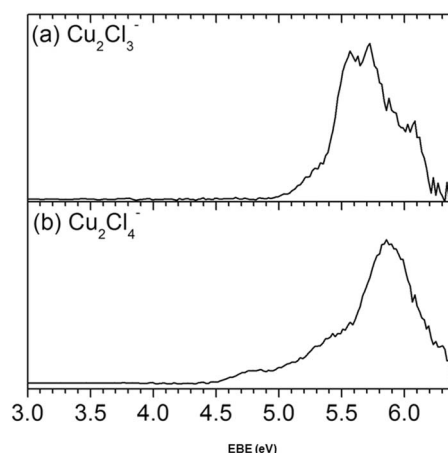


FIG. 5. Photoelectron spectra of Cu_2Cl_n^- ($n = 3$ and 4) cluster anions recorded with 193 nm photons.

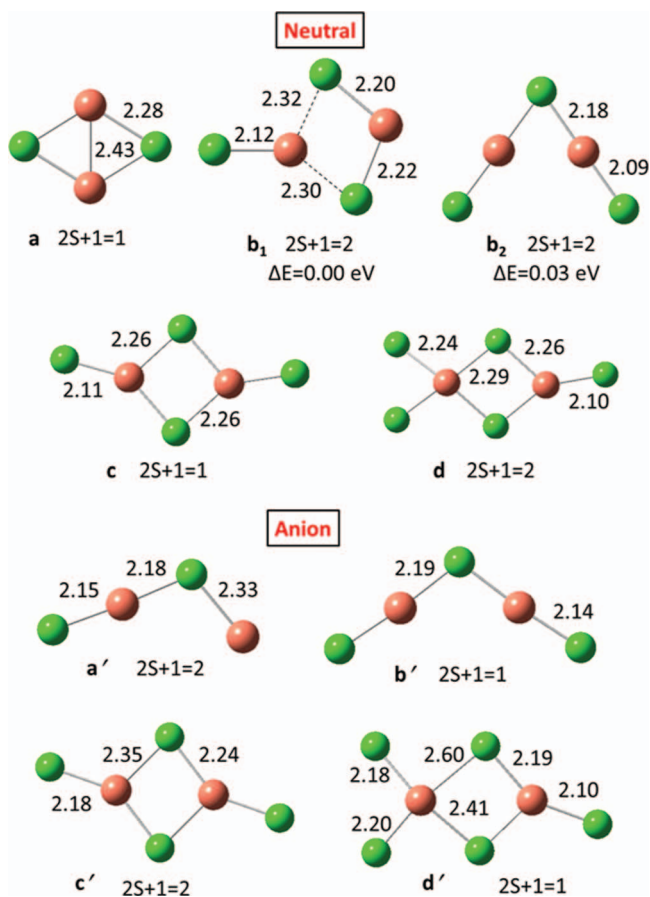


FIG. 6. Optimized geometries of neutral and anionic Cu_2Cl_n ($n = 2-5$) clusters. The green spheres represent chlorine atoms, while the red spheres are copper atoms. All the bond lengths are given in Angstroms.

observed earlier in Na_mCl_n (Ref. 16), $\text{Au}_m(\text{BO}_2)_n$ (Ref. 34), and very recently in Mn_xCl_y (Ref. 35) clusters and predicted theoretically.^{17,36-38} To understand the origin of the superhalogen behavior of these multi-metal clusters, we note that $\text{Cu}_m\text{Cl}_{m+1}$ can be written as $(\text{CuCl})_m\text{Cl}$. Here, Cu exists in the oxidation state of +1. Thus, $\text{Cu}_m\text{Cl}_{m+1}$ clusters behave as a superhalogen, but the core is replaced by CuCl instead of just the Cu atom. Cu has an oxidation state of +1 in Cu_2Cl_3 cluster which can be written as $(\text{CuCl})_2\text{Cl}$. If Cu were to have an oxidation state of +2 in Cu_mCl_n clusters, $(\text{CuCl}_2)_2\text{Cl}$ should behave as a superhalogen and hence should be stable. Note that a similar behavior has been observed in Mn_2Cl_5 (Ref. 30) and theoretically predicted for Mg_2F_5 (Ref. 12) cluster. There is a significant peak for Cu_2Cl_5^- which confirms the possibility of +2 oxidation state of Cu.

The ground state and higher energy geometries of neutral and negatively charged Cu_2Cl_n ($n = 2-5$) clusters are given in Figure 6. The ground state geometries of neutral and anionic Cu_2Cl_2 cluster are different. The neutral Cu_2Cl_2 cluster forms a rhombus structure (C_{2v} symmetry) with Cu–Cl bond lengths of 2.28 Å and Cu–Cu bond length 2.43 Å (Fig. 6, a). The ground state geometry of Cu_2Cl_2^- cluster, on the other hand, is a bent open structure with C_s symmetry (Fig. 6, a'). In this geometry, there are no metal–metal bonds and can be derived from the CuCl_2 cluster (Fig. 1, 2a) with the second Cu atom binding to one of the halogen atoms. Interestingly,

the rhombus structure, which is the ground state in neutral, is 0.89 eV higher in energy than the bent structure. The change in the ground state geometry from a rhombus structure in neutral to a bent structure in anion can be understood from the MO analysis. The LUMO of the neutral Cu_2Cl_2 cluster is twofold degenerate, the addition of an electron to LUMO results in distortion of the structure (breaking of Cu–Cu and Cu–Cl bonds); thereby lifting the symmetry.

We now turn to neutral and anionic Cu_2Cl_3 cluster. The lowest energy geometry (C_s symmetry) of neutral Cu_2Cl_3 cluster can be seen as an extension of neutral Cu_2Cl_2 cluster, where the third Cl atom binds to one of the Cu atoms of the rhombus (Fig. 6, b₁). The addition of this halogen atom caused the breaking of Cu–Cu bond and weakening the two existing Cu–Cl bonds (10% elongation); thereby resulting in a threefold coordination for one of the metal atoms. Another planar isomer (C_{2v} symmetry) in which both the Cu atoms are twofold coordinated is found to be 0.03 eV higher in energy (Fig. 6, b₂). Most importantly, this isomer can be derived from the ground state geometry of Cu_2Cl_2^- cluster. Interestingly, the structural configuration corresponding to the lowest energy geometry of neutral Cu_2Cl_3 cluster is not even a minimum on the potential energy surface of the Cu_2Cl_3^- cluster. The ground state geometry (Fig. 6, b') of Cu_2Cl_3^- corresponds to a bent structure (C_{2v} symmetry), similar to that of the higher energy isomer of neutral Cu_2Cl_3 . A comparison of the NBO charge distributions in the ground state Cu_2Cl_3^- cluster (Fig. 6, b') and the structurally similar Cu_2Cl_3 (Fig. 6, b₂) shows that the extra-electron in the anionic cluster is delocalized over the entire cluster, with 40% distributed over the metal atoms, while the rest 60% over the halogen atoms. Thus, the delocalization of the electron on the entire cluster, as opposed to the positively charged Cu atoms results in the superhalogen behavior of Cu_2Cl_3 cluster, which is discussed in detail below. The ground state geometries of neutral and negatively charged Cu_2Cl_4 cluster (Fig. 6, c and c') can be derived from the lowest energy isomer of Cu_2Cl_3 (Fig. 6, b₁), where the fourth chlorine binds to the low coordinated Cu atom. Cu_2Cl_5 cluster can be considered as an extension of Cu_2Cl_4 , where the fifth chlorine atom binds to one of the Cu atoms, making it fourfold coordinated, while the other Cu atom has a threefold coordination. The neutral and anionic Cu_2Cl_5 clusters are similar to each other (Fig. 6, d and d').

To understand the stability of the Cu_2Cl_n^- ($n = 2-5$) clusters, we have calculated the fragmentation energies of these clusters via different fragmentation channels. Our calculations show that the most preferred channel has CuCl_2^- clusters as the end product. This is because of the high stability of CuCl_2^- cluster. In Fig. 7, we show the fragmentation channels with the required energies for fragmentation. The energy required to dissociate Cu_2Cl_2^- cluster is much less than that of Cu_2Cl_3^- or Cu_2Cl_4^- or Cu_2Cl_5^- cluster. This further explains the observed peaks of Cu_2Cl_3^- and Cu_2Cl_4^- clusters in the mass spectra along with Cu_2Cl_5^- cluster as shown in Fig. 3.

The calculated EA values of Cu_2Cl_n and VDE values of Cu_2Cl_n^- ($n = 2-5$) clusters are given in Table I. The EA of Cu_2Cl_2 is expected to be small. This is because two Cu atoms donate two electrons to complete the p -shell of the

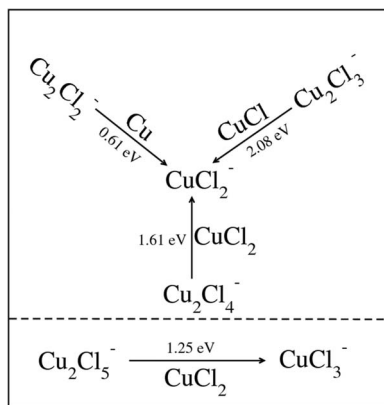


FIG. 7. Fragmentation channels for Cu_2Cl_n^- ($n = 2-5$) clusters are shown to describe the preferred product.

Cl atoms; hence, the added electron goes to neutralize the positive charge on the Cu atom as opposed to being distributed among the Cl atoms. However, as more Cl atoms are added to Cu_2 , the extra electron redistributes itself among the Cl atoms and hence they behave as superhalogens. The computed results agree well with experiment. We also note that the EA of CuCl_3 is larger than that of Cu_2Cl_3 or Cu_2Cl_4 clusters. Average charges on Cu atoms indicate that only 0.38 e and 0.24 e of the extra electron goes to Cu atoms in Cu_2Cl_3^- and Cu_2Cl_4^- clusters, respectively, while 0.64 e of the extra electron goes to the Cu atoms in Cu_2Cl_2^- cluster. Difference between the average charge on Cu atoms in both neutral and anion Cu_2Cl_5 clusters are only 0.06 e of the electronic charge and explain the larger EA.

IV. CONCLUSIONS

In summary, a synergistic study involving density functional theory and PES of the structure and electronic properties of Cu_mCl_n clusters has yielded many interesting results: (1) CuCl_n clusters with $n \geq 2$ are superhalogens with EAs substantially higher than that of Cl, (2) Cu_2Cl_3 and Cu_2Cl_4 also show superhalogen properties where the core is a $(\text{CuCl})_2$ cluster; thus, these superhalogens are different from the conventional superhalogens, (3) the clusters studied show that the oxidation state of Cu can be as high as III, (4) the pronounced peaks observed in the mass spectrum are attributed to the superhalogen property of the clusters, (5) clusters of CuCl_n do exhibit properties that are different from those of CuF_n , and (6) once suitable cations are identified, new salts can be synthesized with strong oxidizing properties.

ACKNOWLEDGMENTS

The experimental work (K.H.B.) was conducted with support by The Defense Threat Reduction Agency. The computational work is supported in part by grants from the

Defense Threat Reduction Agency and U.S. Department of Energy. P.K. acknowledges financial support from Honors College, McNeese State University.

- ¹S. Freza and P. Skurski, *Chem. Phys. Lett.* **487**, 19 (2010).
- ²N. Bartlett, *Proc. Chem. Soc., London* **218** (1962).
- ³N. Bartlett and D. H. Lohmann, *Proc. Chem. Soc., London* **115** (1962).
- ⁴G. L. Gutsev and A. I. Boldyrev, *Chem. Phys.* **56**, 277 (1981).
- ⁵G. L. Gutsev and A. I. Boldyrev, *Chem. Phys. Lett.* **101**, 441 (1983).
- ⁶G. L. Gutsev and A. I. Boldyrev, *Adv. Chem. Phys.* **61**, 169 (1985).
- ⁷D. F. Hunt, G. C. Stafford, Jr., F. W. Crow, and J. W. Russell, *Anal. Chem.* **48**, 2098 (1976).
- ⁸Q. Wang, Q. Sun, and P. Jena, *J. Chem. Phys.* **131**, 124301 (2009).
- ⁹X.-B. Wang, C.-F. Ding, L.-S. Wang, A. Boldyrev, and J. Simons, *J. Chem. Phys.* **110**, 4763 (1999).
- ¹⁰X. B. Wang, L. S. Wang, R. Brown, P. Schwerdtfeger, D. Schroder, and H. Schwarz, *J. Chem. Phys.* **114**, 7388 (2001).
- ¹¹M. Elliot, E. Koyle, A. I. Boldyrev, X.-B. Wang, and L.-S. Wang, *J. Phys. Chem. A* **109**, 11560 (2005).
- ¹²I. Anusiewicz and P. Skurski, *Chem. Phys. Lett.* **358**, 426 (2002).
- ¹³I. Anusiewicz, M. Sobczyk, I. Dabkowska, and P. Skurski, *Chem. Phys.* **291**, 171 (2003).
- ¹⁴C. Sikorska, S. Smuczynska, P. Skurski, and I. Anusiewicz, *Inorg. Chem.* **47**, 7348 (2008).
- ¹⁵G. L. Gutsev, P. Jena, and R. J. Bartlett, *Chem. Phys. Lett.* **292**, 289 (1998).
- ¹⁶A. N. Alexandrova, A. I. Boldyrev, Y.-J. Fu, X. Yang, X.-B. Wang, and L.-S. Wang, *J. Chem. Phys.* **121**, 5709 (2004).
- ¹⁷I. Anusiewicz and P. Skurski, *Chem. Phys. Lett.* **440**, 41 (2007).
- ¹⁸G. L. Gutsev, B. K. Rao, P. Jena, X.-B. Wang, and L.-S. Wang, *Chem. Phys. Lett.* **312**, 598 (1999).
- ¹⁹G. L. Gutsev, P. Jena, H.-J. Zhai, and L.-S. Wang, *J. Chem. Phys.* **17**, 7935 (2001).
- ²⁰J. Yang, X.-B. Wang, X.-P. Xing, and L.-S. Wang, *J. Chem. Phys.* **128**, 201102 (2008).
- ²¹K. Pradhan, G. L. Gutsev, and P. Jena, *J. Chem. Phys.* **133**, 144301 (2010).
- ²²O. Graudejus, S. H. Elder, G. M. Lucier, C. Shen, and N. Bartlett, *Inorg. Chem.* **38**(38), 2503 (1999).
- ²³M. K. Scheller, R. N. Compton, and L. S. Ceederbaum, *Science* **270**, 1160 (1995).
- ²⁴R. Craciun, D. Picone, R. T. Long, S. Li, D. A. Dixon, K. A. Peterson, and K. O. Christe, *Inorg. Chem.* **49** (3), 1056 (2010).
- ²⁵R. Craciun, R. T. Long, D. A. Dixon, and K. O. Christe, *J. Phys. Chem. A* **114**(28), 7571 (2010).
- ²⁶P. Koirala, M. Willis, B. Kiran, A. K. Kandalam, and P. Jena, *J. Phys. Chem. C* **114**, 16018 (2010).
- ²⁷M. J. Frisch, G. N. Trucks, and H. B. Schlegel *et al.*, GAUSSIAN 03, Revision B.04, Gaussian, Inc., Pittsburgh, PA, 2003.
- ²⁸B. D. Becke, *J. Chem. Phys.* **98**, 5648 (1993); C. Lee, W. Yang, and R. G. Parr, *Phys. Rev. B* **37**, 785 (1988).
- ²⁹M. Gerhards, O. C. Thomas, J. M. Nilles, W.-J. Zheng, and K. H. Bowen, *J. Chem. Phys.*, **116**, 10247 (2002).
- ³⁰X. Li, A. Grubisic, S. T. Stokes, J. Cordes, G. F. Gantefoer, K. H. Bowen, B. Kiran, M. Willis, P. Jena, R. Burgert, and H. Schnoekel, *Science* **315**, 356 (2007).
- ³¹A. E. Reed, L. A. Curtiss, and F. Weinhold, *Chem. Rev.* **88**, 899 (1988).
- ³²S. Riedel and M. Kaupp, *Coord. Chem. Rev.* **253**, 606 (2009).
- ³³W. D. Knight, K. Clemenger, W. A. de Heer, W. A. Saunders, M. Y. Chou, and M. L. Cohen, *Phys. Rev. Lett.* **52**, 2141 (1984).
- ³⁴M. Götz, M. Willis, A. K. Kandalam, G. F. Ganteför, and P. Jena, *Chem. Phys. Chem.* **11**, 853 (2010).
- ³⁵M. M. Wu, H. Wang, Y. J. Ko, Q. Wang, Q. Sun, B. Kiran, A. K. Kandalam, K. H. Bowen, and P. Jena, *Angew. Chem. Int. Ed.* **50**, 2568 (2011).
- ³⁶G. L. Gutsev and A. I. Boldyrev, *Chem. Phys. Lett.* **108**, 250 (1984).
- ³⁷M. Sobczyk, A. Sawicka, and P. Skurski, *Eur. J. Inorg. Chem.* 3790 (2003).
- ³⁸C. Sikorska, S. Freza, P. Skurski, and I. Anusiewicz, *J. Phys. Chem. A* **115**, 2077 (2011).